〈일반논문〉
Journal of the Korean Society of Visualization, Vol. 21, No. 3 (23~32), 2023
(Manuscript received : 2023.10.06./Revised : 2023.11.01./Accepted : 2023.11.01.)
DOI:http://dx.doi.org/10.5407/jksv.2023.21.3.023

ISSN 1598-8430 Print
ISSN 2093-808X Online

전기히터의 설계 변수에 따른 순간온수기 열유동 특성 해석

쑨휘* · 김준현** · 성재용†

Analysis of heat and fluid flows in an instant water heater according to design parameters of an electric heat device

Hui Sun*, Joon Hyun Kim** and Jaeyong Sung†

Abstract This study aims to explore the heat transfer and flow phenomena inside an instant water heater and the influence of the design parameters of the water heater on the heating performance was investigated by 3-D numerical simulations considering heat convection. The design parameters are the heating ceramic dimension, the power of the heating device, and the water flow rate. The results show that a reasonable space for the heating device is required to optimize the heating performance. It is desirable to design higher heating device as possible for a given electric power. There exists a critical water flow rate that best meets the heating performance. The change in electric power has no impact on the flow phenomena and heating performance.

Key Words : Instant water heater(순간온수기), Electric heat device(전기가열장치), CFD(전산유체역학), Heat and fluid flow(열유동), Heat convection(대류 열전달)

1. Introduction

Nowadays, energy demand is increasing due to population growth and improved living standards. The hot water supply in daily life is significant energy consumption. In the US, EU, China, and South Africa, energy from water heating accounts for 14-32% of total household energy consumption[1]. Environmentally inefficient residential energy consumption has accelerated greenhouse gas emissions[2-3]. Therefore, reducing energy consumption and improving thermal efficiency for hot water production systems have become very important. How to enhance heat transfer is a factor in the design of hot water production systems[4].

Most papers have focused on optimizing the design of water flow paths and heating elements to improve the thermal efficiency of heating devices. About the water flow paths, Duff and Bradnum[5] proposed a double annulus heating chamber design concept. Sedeh and Khodadadi[6] used baffles to change the water flow patterns. Ahn and Kim[7] designed a jaw in the middle of the heater so that the water could generate a vortex and the heated water was mixed more evenly.

† SeoulTech, Dept. of Mechanical and Automotive Engineering, Professor
E-mail: jysung@seoultech.ac.kr
* SeoulTech, Graduate School, Graduate student
** SeoulTech, NDT Research Center, Research Professor

With regards to the heating elements, Nicoară et al.[8] conducted numerical simulations to improve thermal efficiency by adjusting the position and shape of heating elements. Liu et al.[9] proposed a heater including a double helix tube to increase the heating area and heat transfer rate. Sezai et al.[10] proposed the idea of using dual heating elements and investigated the effect of the heater position on the heating performance. Hegazy and Diab[11] mentioned that the shape of heating devices with the same electric power affects the flow and mixing of hot and cold water.

The purpose of this paper is to investigate the phenomenon of heat and fluid flows inside an instant water heater by 3-D numerical simulations. As design parameters, the open space, height and electric power of the heating device and the water flow were changed. From the results, the effect of the design parameters of the water heater on its performance is discussed. In addition, an optimum condition to achieve a quick and stable outlet temperature is presented.

2. Numerical method

2.1 System design

Fig. 1 shows the 3-D model used for the study, which consists of a coil pipe, an electric heating device, and a water tank. The size of cylindrical water tank is 90 mm in diameter (D) and 110 mm in height (H). The material of the coil pipe is steel, the inner diameter is 5.4 mm, and the thickness is 1 mm. The heating device is made of ceramic material and consists of three rectangular plates fixed to the bottom of the water tank. Cold water enters the pipe from the inlet and then moves to the bottom of the tank through the spiral coil pipe. The water is discharged into the tank through a coil pipe at the bottom. After being heated by the heating device, the heated water is discharged through the top outlet.

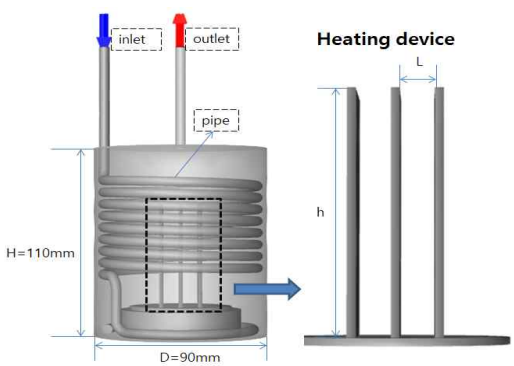

Fig. 1. Schematic of an instant water heater and heating device.

Table 1 shows the physical of the materials involved in this study. For the design parameters, as shown in Table 2, the shape of the heating device (open space (L), ceramic height (h)), electric power (E), and water flow rate (Q) are used. The base design conditions are the open space L = 8 mm, ceramic height h = 60 mm, the water flow rate 50 mL/s, and the electric power E = 5.2 kW. The design parameters of the heating device are non-dimensionalized as shown in Table 3. The open space (L) and ceramic height (h) of the heating device are normalized by the diameter (D) and the height (H) of the water tank, respectively.

Table 1. Physical of materials used.

Material	Property(unit)	Value
Steel	Density (kg/m^3)	8030
	Specific heat (J/kg-K)	502.5
	Thermal conductivity (W/m-K)	16.7
Ceramic	Al_2O_3 Purity (%)	96
	Density (kg/m^3)	3730
	Specific heat (J/kg-K)	880
	Thermal conductivity (W/m-K)	20.9
Water	Density (kg/m^3)	998.2
	Specific heat (J/kg-K)	4182
	Thermal conductivity (W/m-K)	0.6
	Viscosity (kg/m-s)	0.001

Table 2. Parameters of the instant water heater.

	Parameters	Value			
Heating device	Open space(mm), L	4	8	12	16
	Ceramic height(mm), h	40	60	80	
	Power(kW), E	4.2	5.2	6.2	
Water	Flow rate(mL/s), Q	25	50	75	

Table 3. Dimensionless parameters of the heating device.

Parameters	Value			
L/D	0.044	0.089	0.133	0.178
h/H	0.364	0.545	0.727	

2.2 Governing equations and boundary conditions

The flows inside the water heater are assumed to be 3-D unsteady, incompressible, and turbulent. The heat transfer from the heating device to hot water is mainly governed by heat convection. Thus, the governing equations of the fluid flows can be written as follows:

$$\nabla \cdot \vec{u} = 0 \tag{1}$$

$$\rho \frac{\partial \vec{u}}{\partial t} + (\rho \vec{u} \cdot \nabla)\vec{u} = -\nabla p + \mu \nabla^2 \vec{u} + \rho g \beta \Delta T \hat{k} \tag{2}$$

$$\rho c_p \left(\frac{\partial T}{\partial t} + (\vec{v} \cdot \nabla) T \right) = k \nabla^2 T \tag{3}$$

where, $\vec{u}$ is the velocity vector, ρ is the density of the fluid, μ is the dynamic viscosity, g is the acceleration due to gravity, β is the volumetric thermal expansion coefficient, c_p is specific heat, and k is the thermal conductivity of the fluid.

The numerical simulations are conducted using Fluent software. As boundary conditions, velocity is specified at the inlet according to the water flow rate. At the outlet, exit environment is done as atmospheric pressure. In the boundary setting of heating conditions, it is assumed that all electrical energy is converted into thermal energy and simulated the heat source by setting the heat flux to the walls of the heating device. The heat on the wall is transferred to the water in contact with it, and then the heating process is completed through convection between the hot and cold water. To simulate the heat transfer through the pipe wall, a coupling method is applied, where only a thickness is set to allow the conductive heat transfer through the pipe wall. The heat loss on the outside surface of the water tank is ignored, so an adiabatic boundary condition is applied. Initially, the water inside the flow domain is still at a room temperature of 293.15K. When the heater starts to operate, water is supplied by a given flow rate through the inlet pipe with a constant temperature of 293.15K.

2.3 Mesh generation

For this model unstructured tetrahedrons were used to generate the mesh. To prevent the calculation results from being affected, the mesh sizes of the pipes, heating devices, and water outlets were refined, and the irrelevance of the four sets of mesh was verified. Fig. 2 shows the solution results for mesh independence. When the number of mesh increases to 2663319, the results

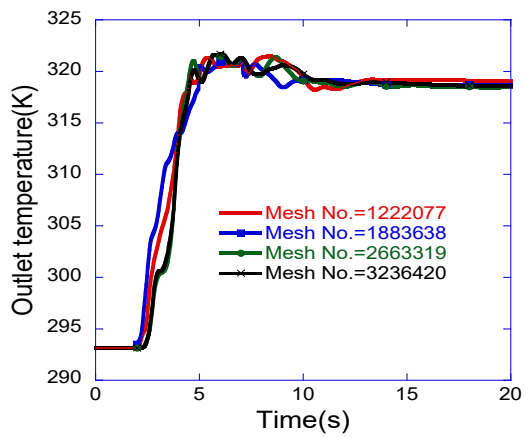

Fig. 2. The effect of the number of meshes on the results.

change is consistent, so the verification is considered passed. In this mesh the element size of both the heating device and the outlet pipe is set to 0.6 mm, and the area around the coil pipe is subdivided to 0.8 mm.

3. Results and discussion

3.1 Effect of the space of the heating device

Fig. 3 shows the changes in outlet water temperature with time for various spaces of the heating device. In this Fig., h/H = 0.545, Q = 50 mL/s, and E = 5.2 kW are used. The outlet temperature rises steeply about 2 ~ 3 s after heating is started. Further heating makes the temperature stabilized at a certain level. The change in the space of the heating device has a meaningful effect on heating. As the space increases, the temperature fluctuation becomes smaller, and the maximum temperature gradually decreases.

Since the water temperature changes varies according to the design parameters, the water temperature is normalized as follows;

$$T^*(t) = \frac{T_o(t) - T_i}{T_{o,th} - T_i} \tag{4}$$

where T* is the dimensionless temperature, $T_o(t)$ is the outlet water temperature, T_i is the inlet water temperature, and $T_{o,th}$ is the final theoretical outlet water temperature, which can be obtained by the following formula:

$$T_{o,th} = \frac{E}{\dot{m}c_p} + T_i \tag{5}$$

where $\dot{m}$ is the mass flow rate of water, c_p is the specific heat of water, and E is the electric power of the heater.

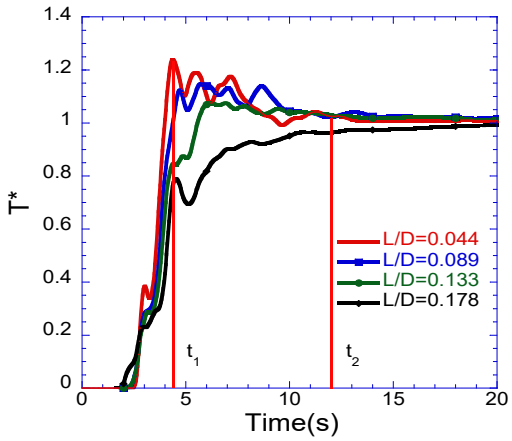

Fig. 3. Variation of the outlet water temperature with time according to the space of the heating device.

To characterize the transient behavior of the outlet temperature, two time (t_1, t_2) are specified. The first time (t_1) is when the peak temperature appears. The second time (t_2) is when the temperature reaches a stable temperature within the fluctuation of 0.5℃.

Fig. 4 shows the temperature contours at the time (t_1) when peak outlet temperature occurs in each case of the given space of the heating device. It is shown that the hot water region is more concentrated in the case of the smaller open space between ceramics. In other words, the temperature distribution becomes more uniform as the space increases. Small space restricts the fluid flow, and the hot water mainly gathers near the heating device to form a local high-temperature area, which causes the temperature gradient to become extremely large.

When the locally high-temperature water goes upward to the outlet pipe, the peak temperature occurs at the outlet. Large temperature gradients cause instability in flow, resulting in significant water temperature fluctuations. On the other hand, the increased open space of the heating device allows more water to pass through the heater

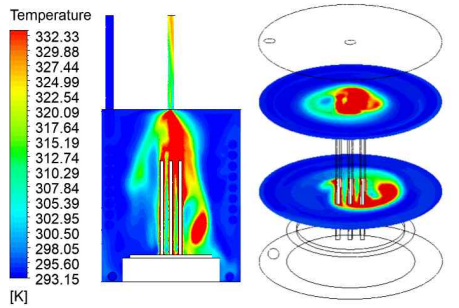

(a) L/D = 0.044

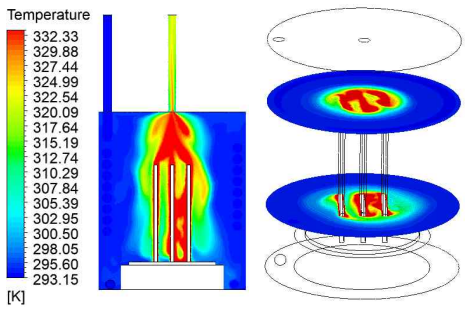

(b) L/D = 0.089

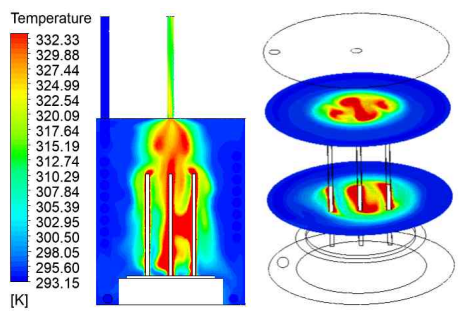

(c) L/D = 0.133

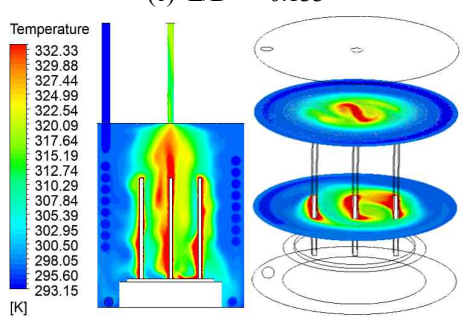

(d) L/D = 0.178

Fig. 4. Temperature contours at the time (t_1) when peak outlet temperature occurs.

region. This results in a more uniform temperature distribution, making small temperature fluctuations

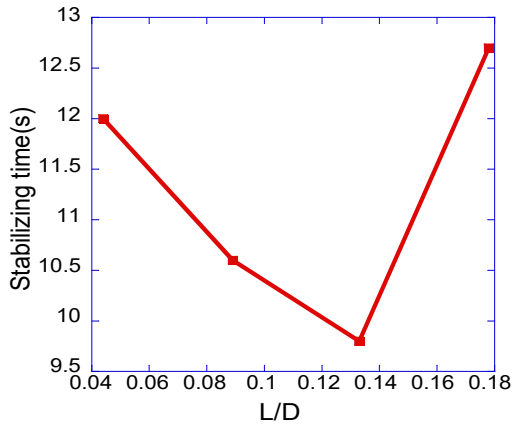

Fig. 5. The time (t_2) required to reach a stable temperature according to the space of the heating device.

in the outlet.

Fig. 5 shows the stabilizing time (t2) required to reach a stable temperature for various spaces of the heating device. As the open space of the heating device increases, the stabilizing time decreases until L/D is 0.133. However, when the L/D is further increased to 0.178, as shown in Fig. 3. In this case, the heating rate is relatively slow, leading to a longer heating time. The stabilizing time is the least at an L/D of 0.133. Therefore, appropriately increasing the space of heating devices can shorten the heating time, but excessively increasing the open space of the heating device can have negative consequences.

3.2 Effect of the height of the heating device

Fig. 6 shows the variation of outlet water temperature with time for various heights of the heating device. In this Fig., L/D = 0.133, Q = 50 mL/s and E = 5.2 kW are used. Note that even though the size of the heating plate increases, the total heat flux is the same by reducing the heat flux per unit area. It is observed that when h/H is 0.727, the water temperature starts to rise as soon as the heater is operated, and there are minimal

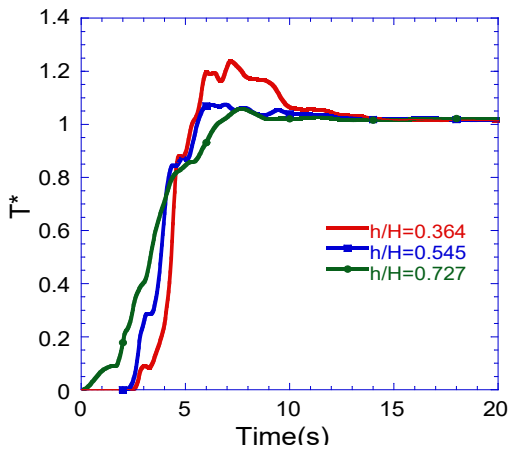

Fig. 6. Variation of the outlet water temperature with time according to the height of the heating device.

fluctuations throughout the heating process. In other cases, the water temperature rose with some delay after turned on. When h/H is 0.545, there are slight temperature fluctuations, and when h/H is 0.364, a higher peak temperature is observed. After further heating, all cases eventually reached a steady state. As the height of the heating device increases, the temperature fluctuation becomes significantly smaller, and the maximum temperature gradually decreases.

The temperature contours at which the peak outlet temperature occurs are shown in Fig. 7 at a given height of the heating device. The increase in the non-dimesionlized height of the heating device reduces the hot region inside the water heater. When the height of the heating device increases, the heating area in contact with water increases, and the heat flux released per unit area decreases. The smaller height of the heating device concentrates heat near the heating device, which leads to higher temperature gradients. The more concentrated hot water inside the tank flows out, which makes a higher peak temperature appear at the outlet. On the contrary, if the height of the heating device is increased, the large heating area

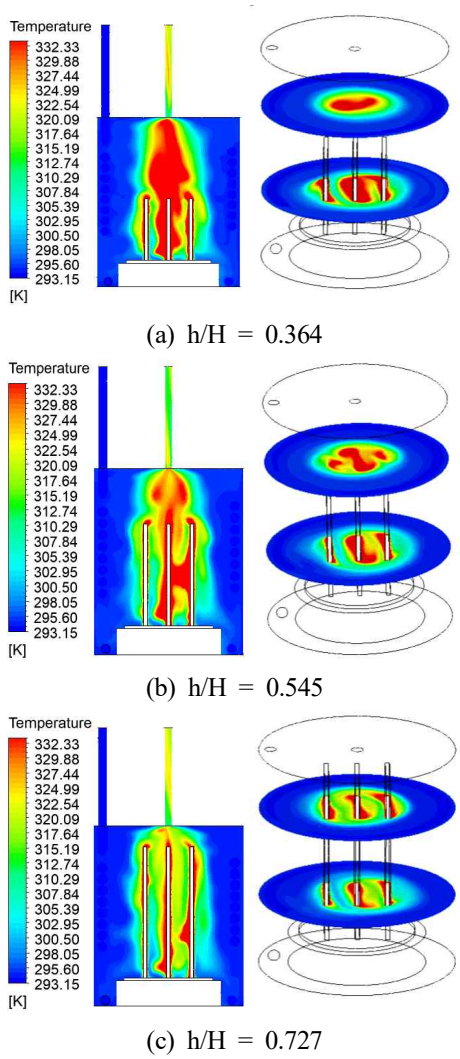

(a) h/H = 0.364

(b) h/H = 0.545

(c) h/H = 0.727

Fig. 7. Temperature contours at the time (t_1) when peak outlet temperature occurs.

makes the same heat transfer to more water, so the heat distribution is more uniform, and the temperature fluctuation is smaller.

Fig. 8 shows the stabilizing time(t_2) required to reach a stable temperature at various non-dimesionlized heights of the heating device. In this Fig., it takes a shorter time for the outlet temperature to be stable as the height of the heating device increases. When the h/H increases from 0.364 to 0.727, the stabilizing time is reduced by 33% from 12.6 s to 8.4 s. Since the

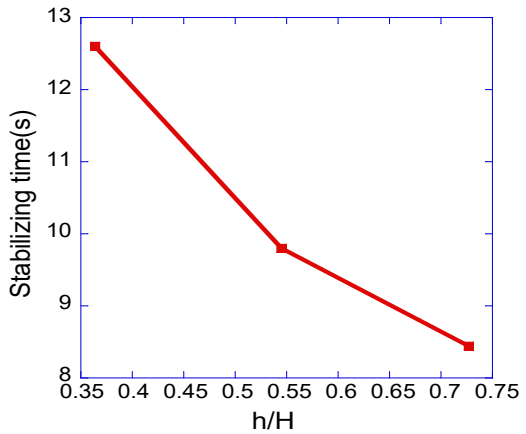

Fig. 8. The time (t_2) required to reach a stable temperature according to the height of the heating device.

increasing height of the heating device has a positive impact on the heating performance, it is desirable to design the heater to be as high as possible for a given electric power.

3.3 Effect of the water flow rate

Fig. 9 shows the temperature variation with time for various water flow rates. In this Fig., L/D = 0.133, h/H = 0.727, and E = 5.2 kW are used. With

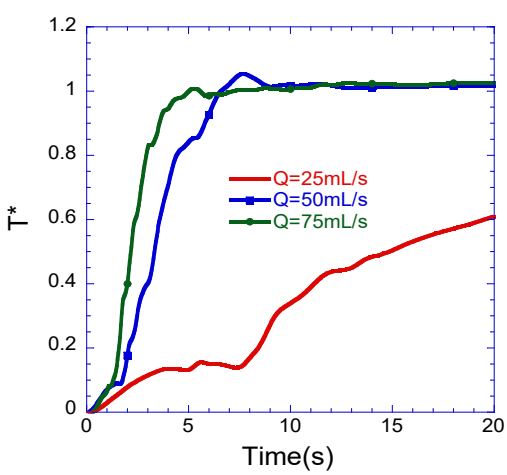

Fig. 9. Variation of the outlet water temperature with time according to the flow rate.

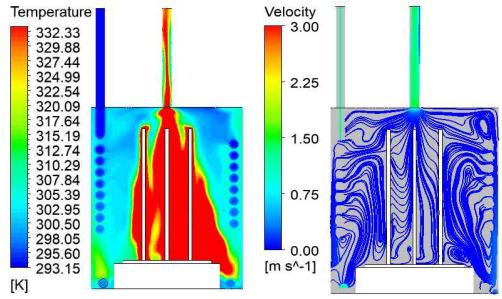

(a) Q = 25 mL/s

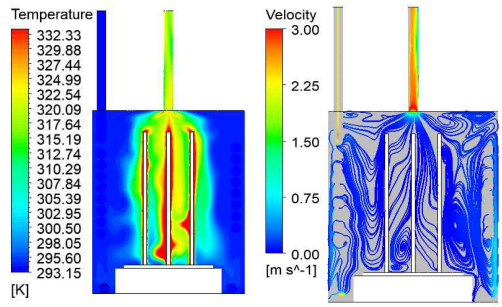

(b) Q = 50 mL/s

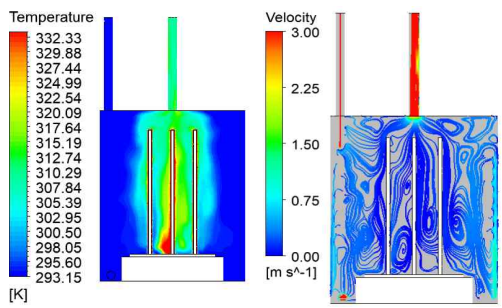

(c) Q = 75 mL/s

Fig. 10. Temperature contours and streamline (2D) at the time (t_1) when peak outlet temperature occurs.

the increase of water flow rate, the rate of the dimensionless temperature-rise increases gradually. The increased water flow rate lowers the absolute outlet water temperature due to the energy balance. In the case of Q = 75 mL/s, the outlet temperature rises sharply as time goes on without significant fluctuation. It reaches a stable temperature at the earliest. For Q = 50 mL/s, the slope of the dimensionless temperature curve becomes relatively flat, and there is a short high-temperature stage before it reaches a steady state. For Q = 25 mL/s, the rate

of temperature-rise is the slowest among the three cases. After the heating starts, the outlet temperature goes up slowly, and it rises faster around t = 7.6 s. Nevertheless, it takes longer to reach a steady state.

Fig. 10 shows the temperature contours and streamlines for water at the time (t_1) when the peak outlet temperature occurs for the given water flow rate. With the increase in water flow rate, the temperature difference between the water tank and the final outlet water temperature gradually decreases. This is because the greater the flow rate, the more water contacts the heating device per unit time. This means the same heat amount is transferred in more water, causing less water temperature rise. As the water flow rate decreases, the water stays in the water heater for a longer time and has more time to absorb heat, so the outlet water temperature becomes higher. In addition, as the water flow rate increases, more vortices are generated, thereby enhancing the convective heat transfer within the fluid. This is the reason for the different temperature-rise rates.

Fig. 11 shows the time required for stable temperature by varying the water flow rate. The results show that the higher the water flow rate, the shorter the time it takes for the temperature to be stabilized. At a low flow rate, increasing the flow rate significantly reduces the stabilization time. However, above a certain flow rate, the decrease in stabilization time is not significant. Since the increased flow rate reduces the final outlet temperature, there exists a critical water flow rate that induces an optimum operating condition for the given design parameters of the instant water heater.

3.4 Effect of the electric power

Fig. 12 shows the temperature variation with time for various electric powers. In this Fig., L/D = 0.133, h/H = 0.727, and Q = 50 mL/s are used. The time history of the dimensionless outlet temperature is the same regardless of the electric power. The increased electric power makes the absolute outlet water temperature higher due to the energy balance. It means that the change in electric power has no effect on the flow itself except for the temperature difference.

Fig. 13 shows the temperature contours at the time (t_1) when the peak outlet temperature occurs for the given electric power. As the electric power increases, the overall temperature inside the water heater increases, but there is no significant difference in the heat

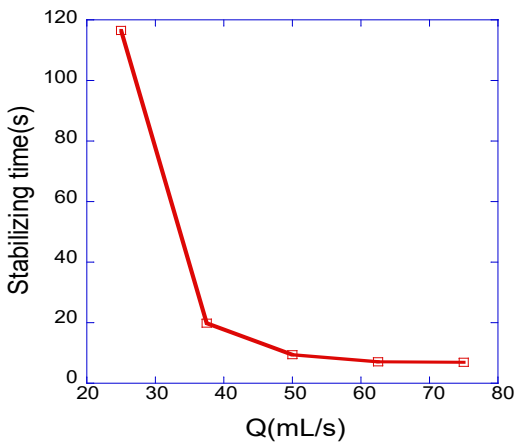

Fig. 11. The time (t_2) required to reach a stable temperature according to the water flow rate.

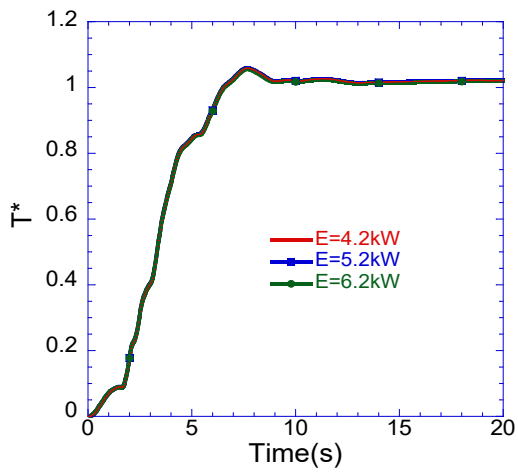

Fig. 12. Variation of the outlet water temperature with time according to the electric power.

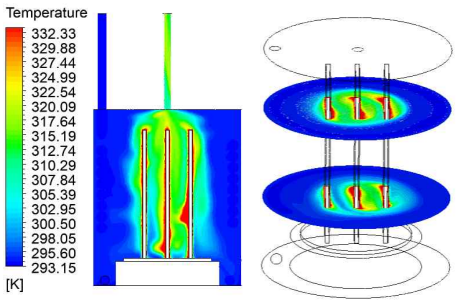

(a) E = 4.2 kW

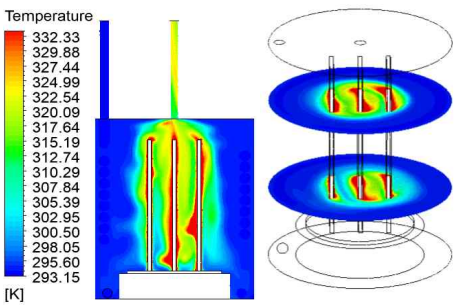

E = 5.2 kW

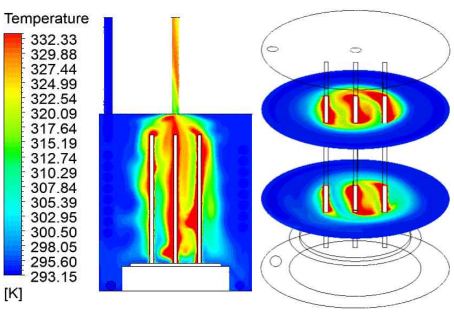

E = 6.2 kW

Fig. 13. Temperature contours at the time (t_1) when peak outlet temperature occurs.

distribution. This shows that the change in electric power only affects the final outlet water temperature.

4. Conclusions

The heat and fluid flow in an instant water heater were numerically simulated according to the design parameters of an electric heating device. Design parameters are open space, ceramic height, electric power of the heating device, and the water flow rate. From the results, the following conclusions were drawn:

The reasonable space of the heating device is of great importance for optimizing the heating performance. An appropriate increase in open space between ceramics for the heating device can reduce the time required to reach a stable temperature, but an excessive increase can have negative consequences.

An increase in the ceramic height of the heating device has a positive effect on the heating performance. As the height of the heating device increases, the outlet temperature is stabilized faster. It is desirable to design a high-heating device for a given electric power.

Increasing water flow can shorten the time required for the stabilizing temperature but lower the outlet water temperature. Thus, there exists a critical water flow rate that best meets the heating performance.

The change in electric power only affects the outlet water temperature and has no effect on flow phenomena and heating performance.

References

1) Ibrahim, O., Fardoun, F., Younes, R. and Louahlia-Gualous, H., 2014, "Review of water-heating systems: General selection approach based on energy and environmental aspects," Building and Environment, Vol.72, pp. 259-286.
2) Li, G. and Du, Y., 2018, "Performance investigation and economic benefits of new control strategies for heat pump-gas fired water heater hybrid system," Applied Energy, Vol.232, pp. 101-118.
3) Pérez-Lombard, L., Ortiz, J., Pout, C., 2008, "A review on buildings energy consumption information," Energy and Buildings, Vol.40(3), pp. 394-398.
4) Fan, J. F., Ding, W. K., Zhang, J. F., He, Y. L. and Tao, W. Q., 2009, "A performance

evaluation plot of enhanced heat transfer techniques oriented for energy-saving," International Journal of Heat and Mass Transfer, Vol.52(1-2), pp. 33-44.
5) Duff, C. A. and Bradnum, C., 2013, "Design of a domestic water heating system to save water and electricity," Proceedings of the 21st Domestic Use of Energy Conference, pp. 1-6.
6) Sedeh, M. M. and Khodadadi, J. M., 2013, "Energy efficiency improvement and fuel savings in water heaters using baffles," Applied energy, Vol.102, pp. 520-533.
7) Ahn, S. S. and Kim, W. H., 2016, "Design and verification of ceramic heating element-based tankless instant electric water heater," Journal of the Institute of Electronics and Information Engineers, Vol.53(11), pp. 151-159.
8) Nicoară, M., Răduţă, A., Cucuruz, L. R. and Locovei, C., 2010, "Numerical simulation of fluid flow and heat transfer in a water heater," Proceedings of the 3rd WSEAS International Conference on Finite Differences-Finite Elements-Finite Volumes-Boundary Elements, pp. 98-105.
9) Liu, Z., Xu, K., Qi, L., Pan, H., Zhang, Z., Pan, Y. and Zeng, Y., 2019, "A high efficiency electric heater based on dual-helical tube and screw-tape for instant water heating," Applied Thermal Engineering, Vol.160, 114018.
10) Sezai, I., Aldabbagh, L. B. Y., Atikol, U. and Hacisevki, H., 2005, "Performance improvement by using dual heaters in a storage-type domestic electric water-heater," Applied Energy, Vol.81(3), pp. 291-305
11) Hegazy, A. A. and Diab, M. R., 2002, "Performance of an improved design for storage-type domestic electrical water-heaters," Applied Energy, Vol.71(4), pp. 287-306.